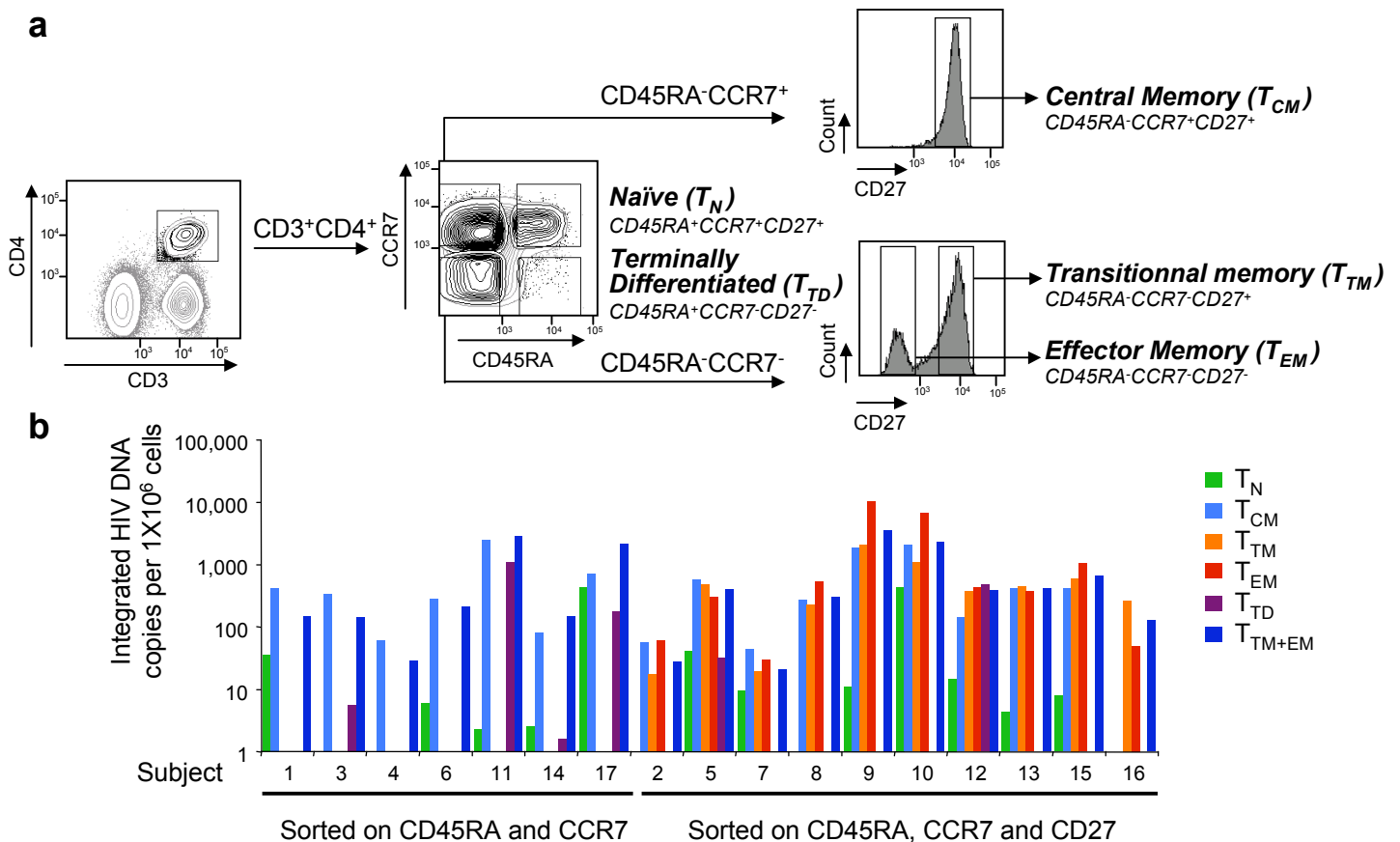


Supplementary information

HIV reservoir size and persistence are driven by T-cell survival and homeostatic proliferation.

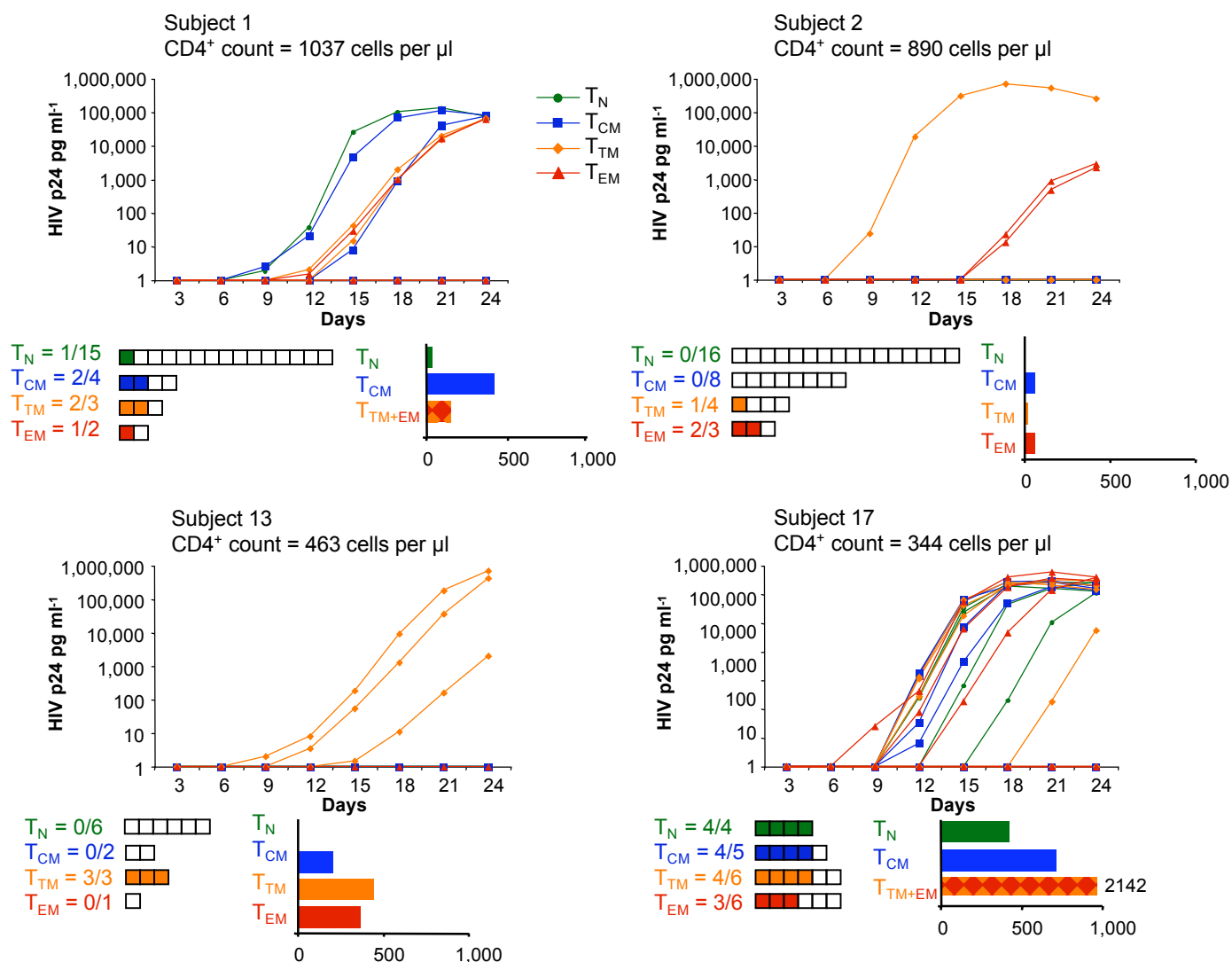
Chomont, N., M. El Far, P. Ancuta, L. Trautmann, F. A. Procopio, B. Yassine-Diab, G. Boucher, M. R. Boulassel, G. Ghattas, J. M. Brechley, Timothy W. Schacker, B. J. Hill, D. C. Douek, J. P. Routy, E. K. Haddad, and R. P. Sékaly

Supplementary Figure 1. Gating strategy and quantification of integrated HIV DNA in sorted CD4⁺ T-cell subsets.



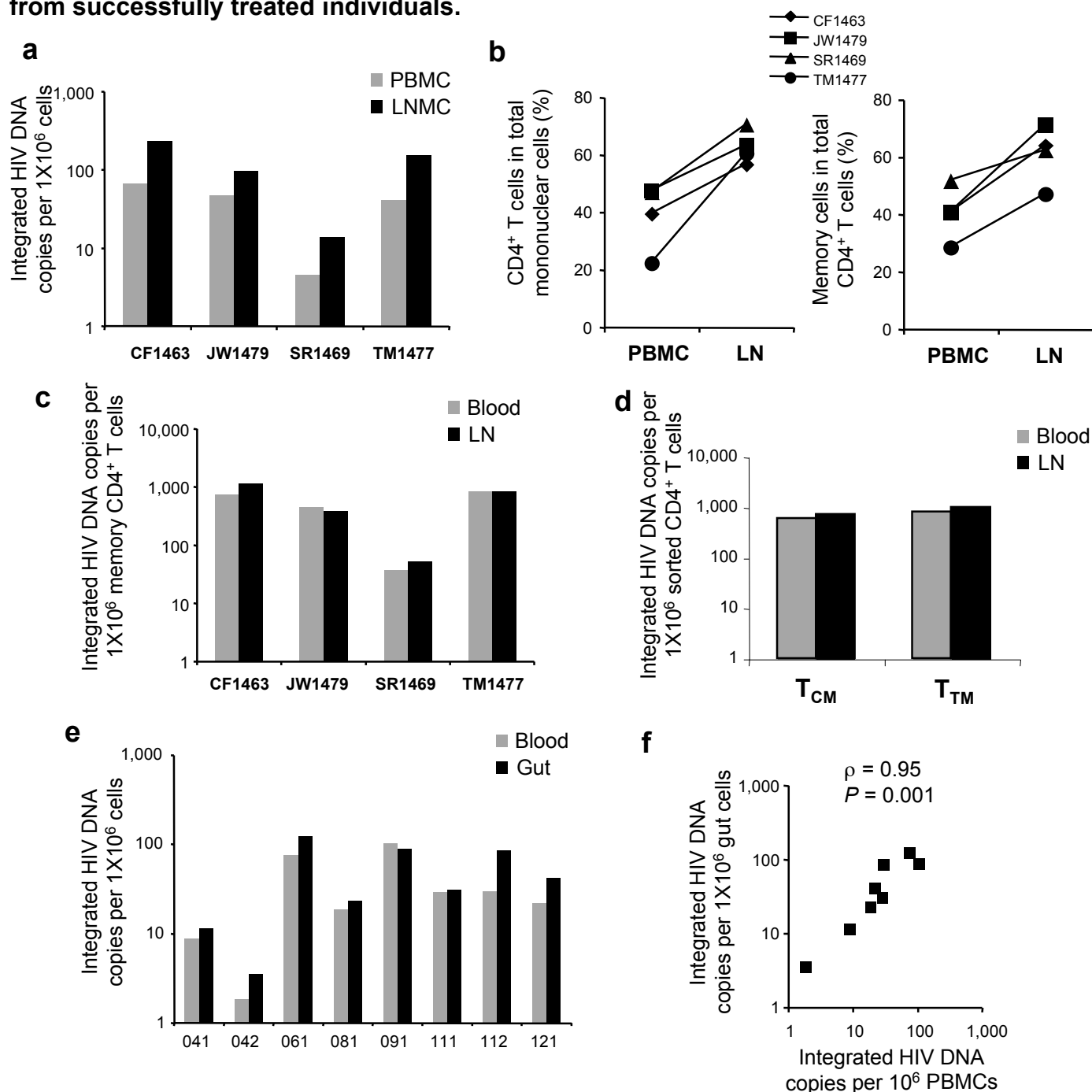
Supplementary Figure 1. Gating strategy and quantification of integrated HIV DNA in sorted CD4⁺ T-cell subsets. (a) CD4⁺ T-cell subsets were isolated after staining with the antibodies indicated in the figure by polychromatic flow cytometry. CD4⁺ T-cells were sorted according to the expression of CD45RA, CCR7 and CD27. CD27 allows to distinguish between T_{TM} (CD45RA⁻CCR7⁻CD27⁺) and T_{EM} (CD45RA⁻CCR7⁻CD27⁻), while all T_{CM} express high levels of CD27 (CD45RA⁻CCR7⁺CD27⁺). PBMC staining from a representative HIV-infected HAART-treated individual is shown. (b) Frequencies of cells harboring integrated HIV DNA in CD4⁺ T-cell subsets from 17 aviremic subjects. Results are expressed as the HIV copy number in 1X10⁶ cells of a given subset.

Supplementary Figure 2. HIV production following activation of CD4⁺ T-cell subsets.



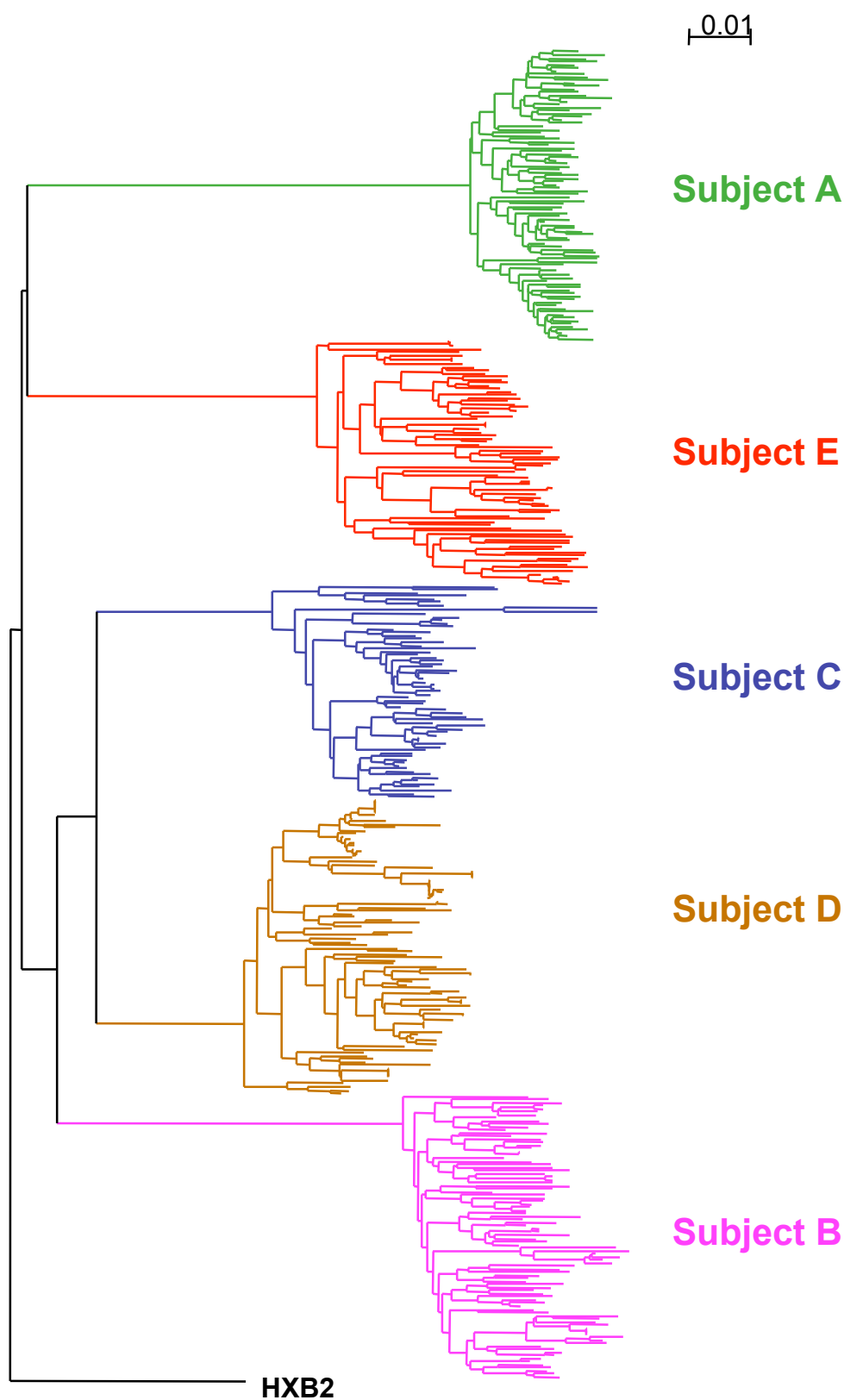
Supplementary Figure 2. HIV production following activation of CD4⁺ T-cell subsets. HIV production was monitored by p24 quantification after PHA/IL-2 stimulation of sorted CD4⁺ T-cell subsets from 4 individuals with undetectable viral load. Replicates of 5×10^5 CD4⁺ T-cells from each subset were stimulated in these conditions. As the number of sorted cells depends on the absolute CD4⁺ count and on the frequency of each subset in the subjects, we were able to purify 0.5 to 8×10^6 cells of each subset (1 to 16 independent stimulations). For each subset, the number of positive wells is represented by filled squares. Integrated HIV DNA copy number was determined in all subsets by *alu* PCR in parallel. For subjects 1 and 17, quantification of integrated HIV DNA is given for T_{TM+EM} because the CD27 antibody was not used in all sorting experiments. In subject 1, we recovered infectious virus from all CD4⁺ T-cell subsets containing integrated HIV DNA. In subject 2, the extremely low frequency of CD4⁺ T-cells harboring integrated HIV DNA explains the small numbers of p24 positive wells ($n = 3/31$) observed after stimulation. The limited number of T_{CM} and T_{EM} cells purified from subject 13 (2 and 1 stimulation, respectively) did not allow us to recover infectious virus from these subsets. Conversely, we were able to recover infectious virus from all T-cell subsets in an individual displaying a high frequency of CD4⁺ T-cells harboring integrated HIV DNA (subject 17).

Supplementary Figure 3. Similar infection frequencies in lymphoid tissues and blood from successfully treated individuals.



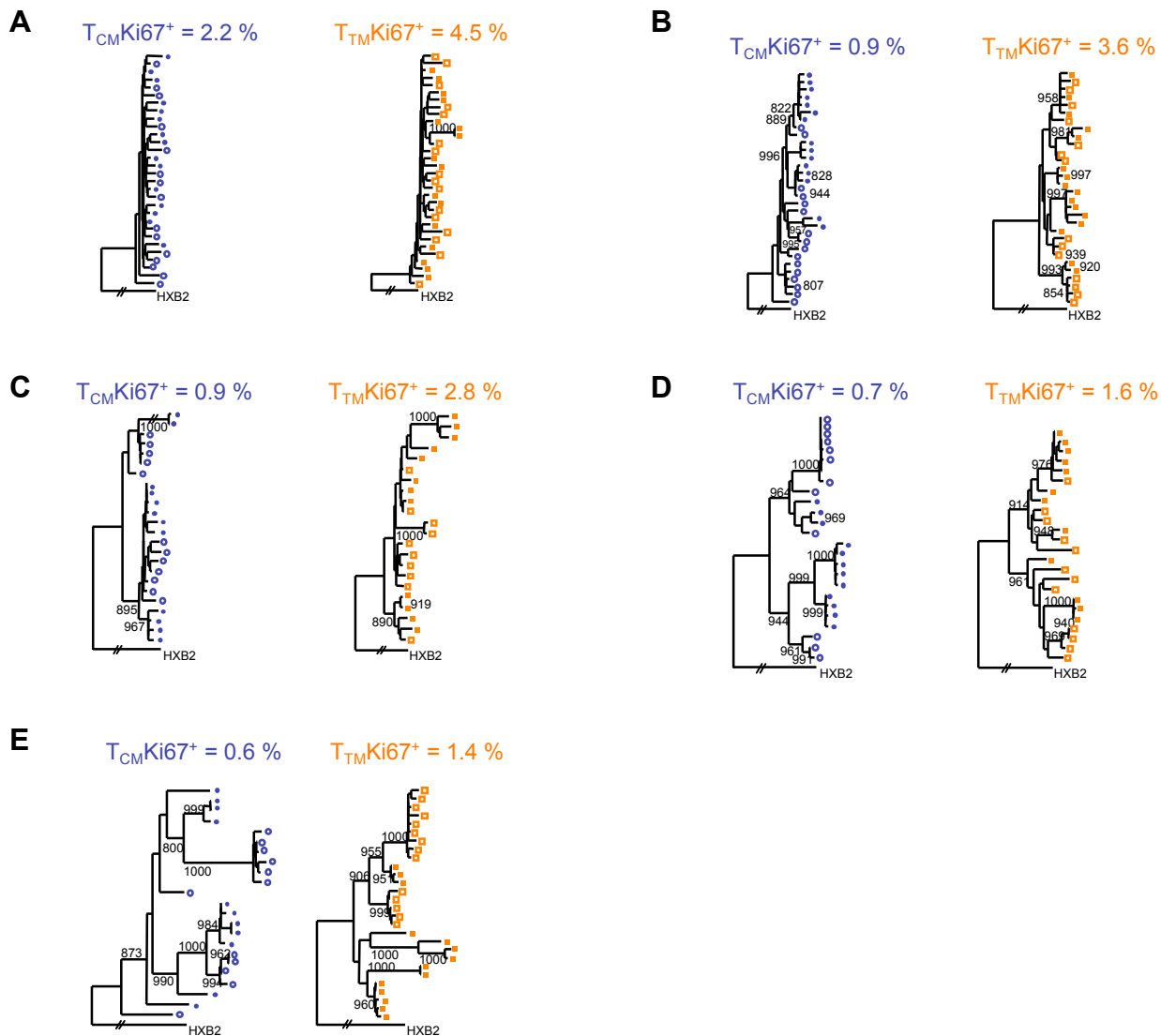
Supplementary Figure 3. Similar infection frequencies in lymphoid tissues and blood from successfully treated individuals. (a) Frequencies of CD4⁺ T-cells harboring HIV integrated DNA in PBMC and matched LNMC. (b) Percentages of CD4⁺ T-cells in PBMC and LN (left panel) and percentage of memory CD4⁺ T-cells within the CD4⁺ compartment (right panel). (c) Frequencies of memory CD4⁺ T-cells harboring HIV integrated DNA in PBMC and matched LN. Results were obtained from infection frequencies in 1×10^6 PBMC and LNMC after correcting for the relative frequency of memory CD4⁺ T-cells in each compartment. (d) Frequencies of cells harboring integrated HIV DNA in sorted T_{CM} and T_{TM} from LN and blood of a successfully treated subject. (e) Frequencies of cells harboring HIV integrated DNA in PBMC and cells from the GI tract in 8 successfully treated individuals. (f) Correlation between the frequencies of cells harboring HIV integrated DNA in PBMC and matched gut biopsies.

Supplementary Figure 4. Phylogenetic relationship of viral clones from 5 individuals.



Supplementary Figure 4. Phylogenetic relationship of viral clones from 5 individuals. The unrooted neighbor-joining tree was obtained from the alignment of V1-V3 DNA sequences. The horizontal branches reflect the relative genetic distances between sequences. HXB2 sequence was included as a control.

Supplementary Figure 5. Evolution of viral sequences in 5 virally suppressed subjects.



Supplementary Figure 5. Evolution of viral sequences in 5 virally suppressed subjects.

Phylogenetic trees derived from HIV sequences obtained from T_{CM} and T_{TM} cells of 5 aviremic subjects (subjects A-E) at first and second time points (closed vs filled symbols, respectively). Percentages of T_{CM} and T_{TM} expressing the Ki67 proliferation marker are indicated.

Supplementary Table 1. Profiles of 34 virally suppressed individuals.

| Patient number ¹ | Plasma HIV RNA ² (copies/ml) | CD4+ cell count (cells/mm ³) | CD8+ cell count (cells/mm ³) | Treatment ³ | Duration of HIV infection (months) ⁴ | Time of aviremia (months) ⁵ | HIV reservoir size ⁶ |
|-----------------------------|---|--|--|------------------------|---|--|---------------------------------|
| 1 | <50 | 1037 | 438 | EFV, IDV | 54 | 46 | 85 |
| 2 | <50 | 890 | 673 | 3TC, AZT, NEV | 57 | 42 | 36 |
| 3 | <50 | 799 | 1727 | 3TC, d4T, NEV | 62 | 33 | 159 |
| 4 | <50 | 691 | 631 | 3TC, AZT, IDV | 74 | 67 | 23 |
| 5 | <50 | 671 | 1120 | 3TC, ABC, LPV, RIT | 242 | 64 | 492 |
| 6 | <50 | 662 | 1051 | d4T, ddI, EFV | 18 | 13 | 258 |
| 7 | <50 | 602 | 767 | 3TC, ABC, SQV | 158 | 53 | 120 |
| 8 | <50 | 599 | 923 | 3TC, AZT, EFV | 86 | 46 | 317 |
| 9 | <50 | 563 | 613 | 3TC, AZT, IDV | 86 | 71 | 1408 |
| 10 | <50 | 552 | 715 | 3TC, d4T, ATZ | 139 | 56 | 567 |
| 11 | <50 | 529 | 690 | 3TC, d4T, DEL | 49 | 11 | 562 |
| 12 | <50 | 510 | 765 | 3TC, AZT, RIT | 61 | 52 | 151 |
| 13 | <50 | 463 | 757 | 3TC, ABC, EFV | 152 | 20 | 736 |
| 14 | <50 | 443 | 322 | 3TC, AZT, LPV, RIT | 18 | 12 | 44 |
| 15 | <50 | 424 | 461 | 3TC, d4T, DEL | 84 | 46 | 416 |
| 16 | <50 | 356 | 629 | 3TC, AZT, ABC | 34 | 6 | 115 |
| 17 | <50 | 344 | 642 | 3TC, d4T, NEV | 59 | 44 | 1135 |
| 18 | <50 | 883 | 333 | EFV, IDV | 86 | 78 | 60 |
| 19 | <50 | 834 | 527 | TDF, NEV, ATZ, RIT | 38 | 25 | 10 |
| 20 | <50 | 825 | 487 | 3TC, AZT, EFV | 16 | 9 | 90 |
| 21 | <50 | 809 | 537 | 3TC, d4T, IDV | 71 | 69 | 10 |
| 22 | <50 | 731 | 413 | 3TC, AZT, EFV | 51 | 22 | 155 |
| 23 | <50 | 688 | 1273 | 3TC, AZT, EFV | 100 | 59 | 242 |
| 24 | <50 | 663 | 333 | TDF, NEV, ATZ, RIT | 55 | 43 | 10 |
| 25 | <50 | 650 | 392 | 3TC, d4T, IDV | 64 | 61 | 10 |
| 26 | <50 | 604 | 1281 | 3TC, AZT, IDV | 53 | 35 | 918 |
| 27 | <50 | 501 | 278 | 3TC, d4T, IDV | 90 | 87 | 10 |
| 28 | <50 | 499 | 602 | 3TC, d4T, ATZ | 155 | 72 | 352 |
| 29 | <50 | 492 | 582 | 3TC, ABC, ATZ, RIT | 170 | 66 | 103 |
| 30 | <50 | 463 | 376 | 3TC, d4T, NFV | 20 | 9 | 31 |
| 31 | <50 | 434 | 583 | 3TC, ABC, EFV | 165 | 34 | 186 |
| 32 | <50 | 396 | 645 | 3TC, AZT, ABC | 70 | 42 | 40 |
| 33 | <50 | 337 | 380 | 3TC, AZT, EFV | 76 | 68 | ND |
| 34 | <50 | 235 | 399 | 3TC, d4T, NEV | 94 | 78 | 817 |
| Mean | <50 | 594 | 657 | | 83 | 45 | 293 |

¹Quantifications of integrated HIV DNA in sorted CD4 T cell subsets were performed in cells from patients 1 to 17.

²Viral load were measured by the Amplicor HIV-1 monitor ultrasensitive Method (Roche), with a detection limit of 50 copies/ml of plasma.

³ Anti-retroviral therapy: 3TC, lamivudine; ABC, abacavir; AZT, zidovudine; d4T, stavudine; ddI, didanosine; TDF, tenofovir; DEL, delavirdine; EFV, efavirenz; ATZ, atazanavir; IDV, indinavir; LPV, lopinavir; NFV, nelfinavir; NEV, nevirapine; RTV, ritonavir; SQV, saquinavir

⁴ Calculated as the time between the first time point with undetectable viral load and the date of leukapheresis.

⁵ Calculated as the time between infection and the date of leukapheresis.

⁶ Integrated HIV DNA copy numbers in 10⁶ CD4 T cells. ND: not determined.

Supplementary Table 2. Profiles of 5 subjects followed longitudinally.

| | Plasma HIV RNA (copies/ml) ¹ | CD4+ cell count (cells/mm ³) | CD8+ cell count (cells/mm ³) | Treatment ¹ | CD4+ Ki67+ cells (%) | Duration of HIV infection (months) ¹ | Time of aviremia (months) ¹ | Time between time points (months) ¹ |
|---|---|--|--|------------------------|-------------------------|---|--|--|
| A | <50 | 344 | 642 | 3TC, d4T, NEV | 2.4 | 59 | 44 | 35 |
| | <50 | 235 | 399 | 3TC, d4T, NEV | 3.5 | 94 | 78 | |
| B | <50 | 529 | 690 | 3TC, d4T, DEL | 1.5 | 49 | 11 | 35 |
| | <50 | 424 | 461 | 3TC, d4T, DEL | 1.9 | 84 | 46 | |
| C | <50 | 1037 | 438 | EFV, IDV | 1.0 | 54 | 46 | 32 |
| | <50 | 883 | 333 | EFV, IDV | 1.5 | 86 | 78 | |
| D | <50 | 599 | 923 | 3TC, AZT, EFV | 1.6 | 86 | 46 | 14 |
| | <50 | 688 | 1273 | 3TC, AZT, EFV | 1.4 | 100 | 59 | |
| E | <50 | 463 | 757 | 3TC, ABC, EFV | 1.4 | 152 | 20 | 14 |
| | <50 | 434 | 583 | 3TC, ABC, EFV | 1.1 | 165 | 34 | |

¹ Same as in Supplementary Table 1.

² Percentage of total CD4 T cell expressing the Ki67 nuclear antigen assessed by flow cytometry.